



UNITED STATES MILITARY ACADEMY
WEST POINT



Distributed Sensor Array for Space Weather Characterization

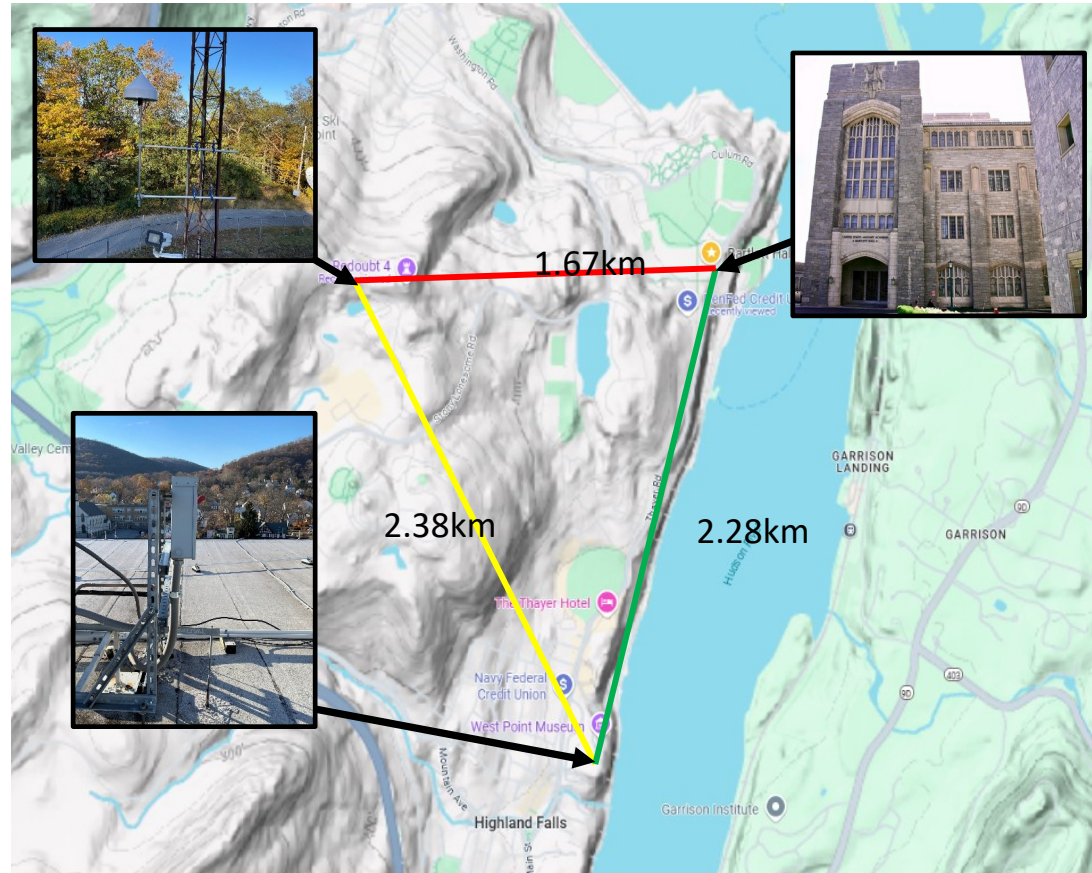


By: CDTs Daniel Klotz
Aaron Jeronimo-Monarca,
Sidharth Hegde,
Preston Poirier
Advisors: COL Diana Loucks,
Dr. Jason Derr

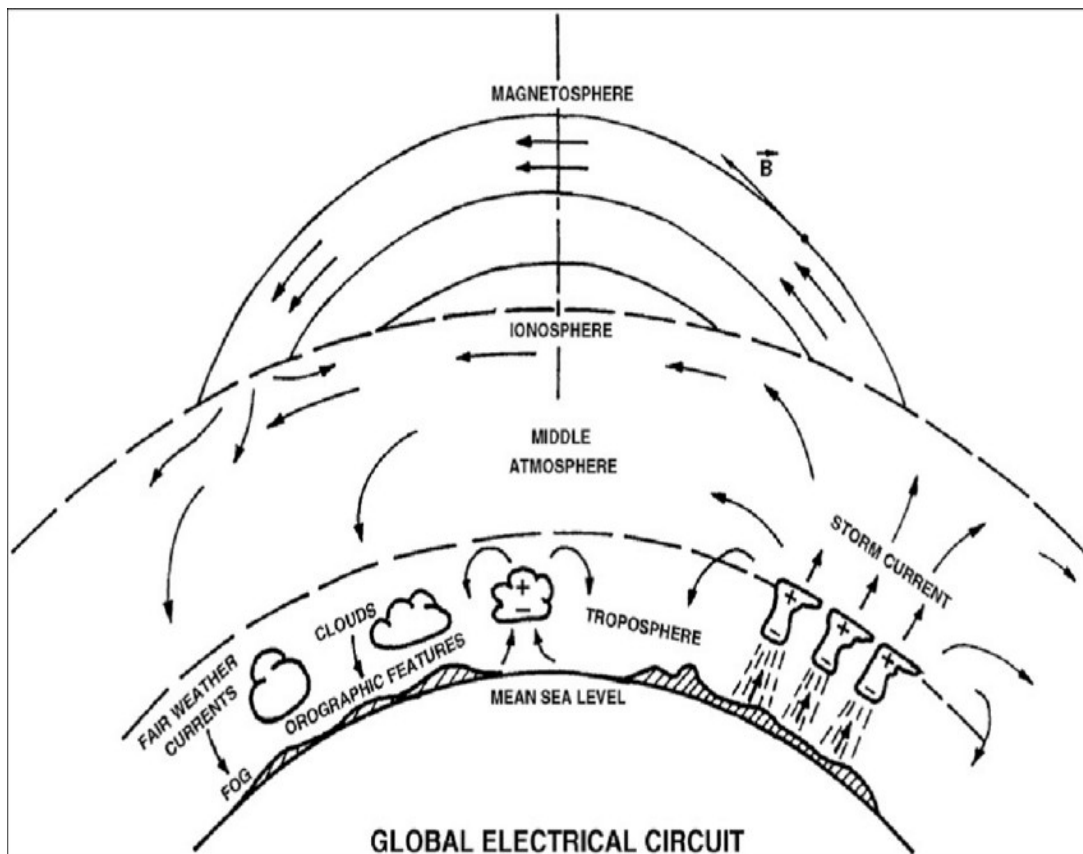




- Background
- Problem Statement
- Current Status
- Project Schedule
- End State



BLUF: The goal of this project is to construct a distributed sensor array on West Point property to measure and characterize the ionosphere. This data will be recorded, analyzed, and used to contribute to the body of mid-latitude ionospheric research (a relatively smaller body compared to what has been done in the polar regions).

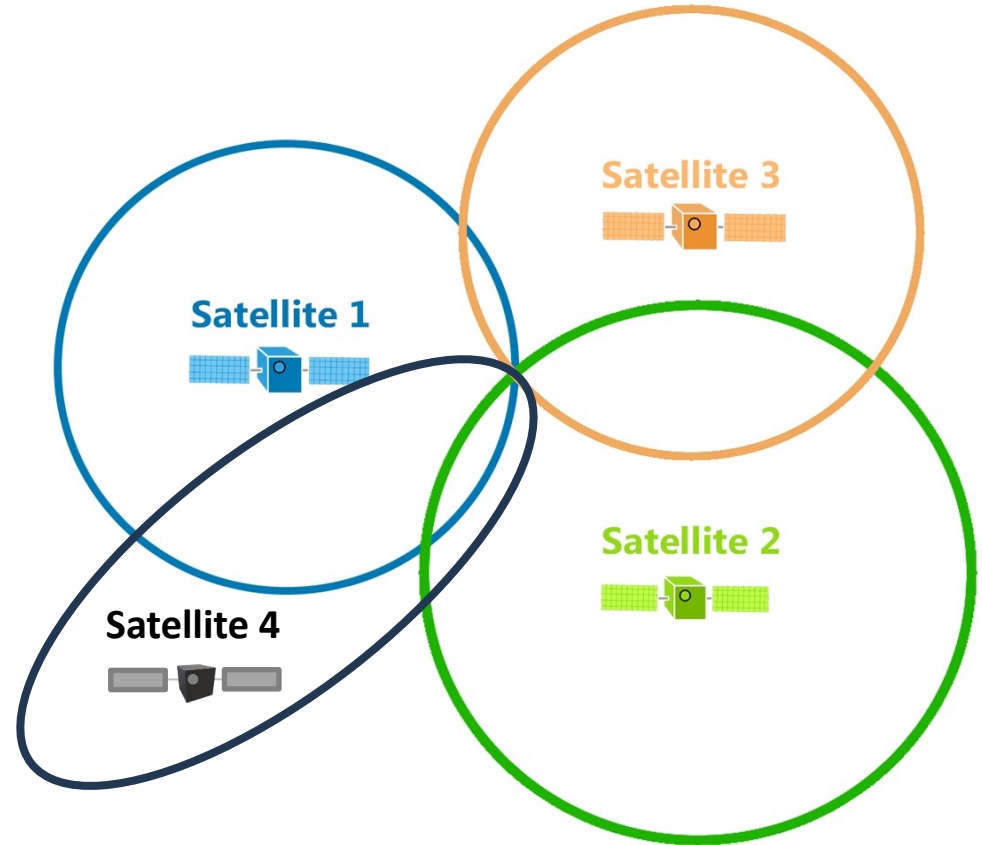
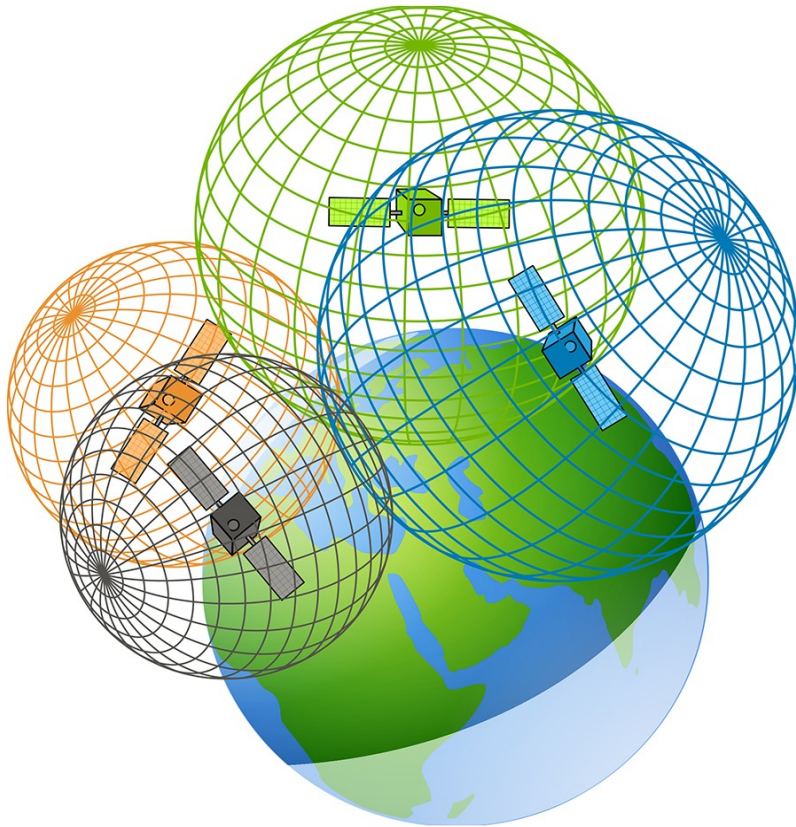


Global Electric Current

- Charge moves from Ionosphere to Earth's surface along magnetic currents
- Fair weather potential difference $\sim 100\text{V/m}$ at $\sim 7.4\text{ Hz}$
- Terrestrial weather increases potential difference
- TIDs in the Ionosphere affect the conductivity



Global Navigation Satellite System

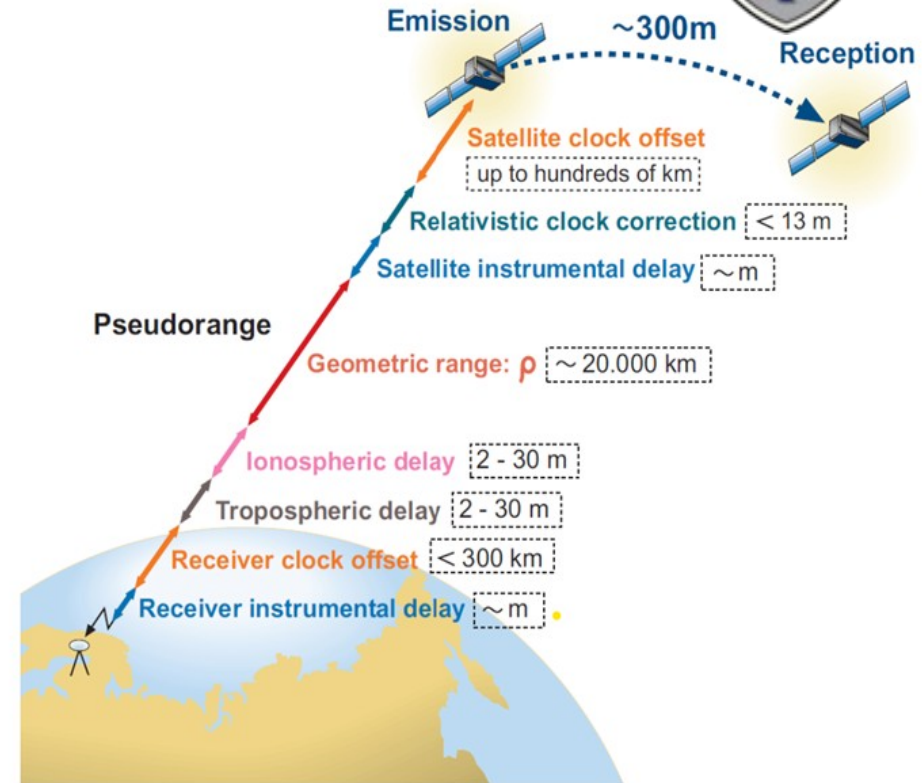




Pseudorange Offset

When passing through the atmosphere, GNSS signals are affected by various phenomena called offsets.

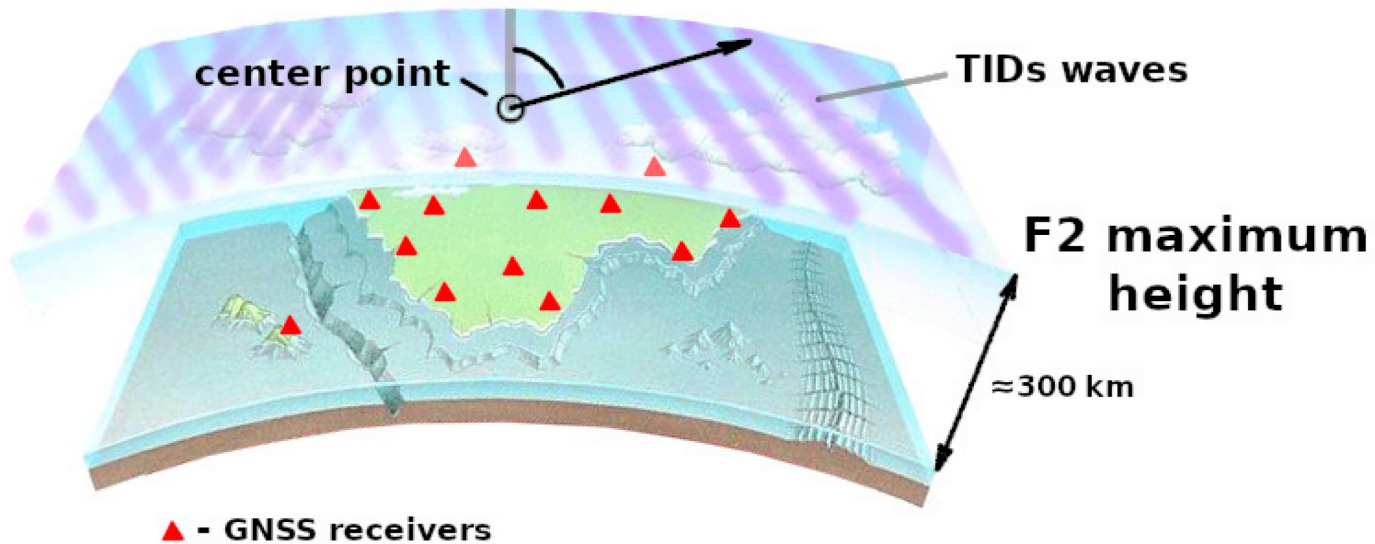
- These alter the data received, and can introduce error in the position solution calculated



Pseudorange

$$p = \rho + d_p + c(dt - dT) + d_{ion} + d_{trop} + \epsilon_{mp} + \epsilon_p$$

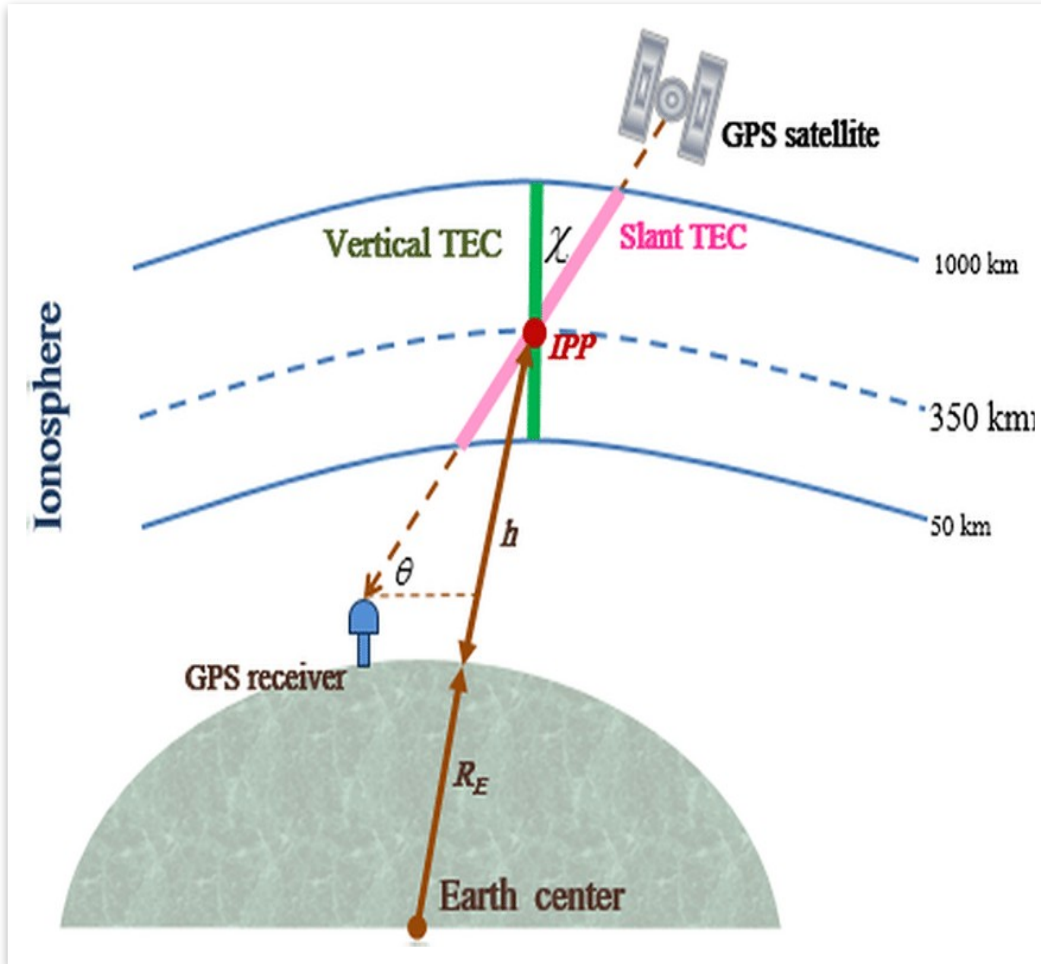




TID Scale	Medium Scale	Large Scale
Wave Size	100-1000 km	>1000 km
Propagation Speed	100-300 m/s	300-1000 m/s



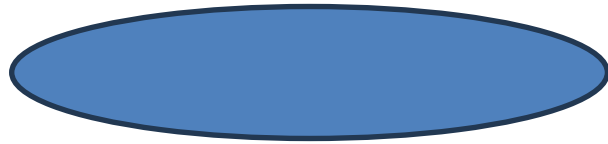
Total Electron Content (TEC)



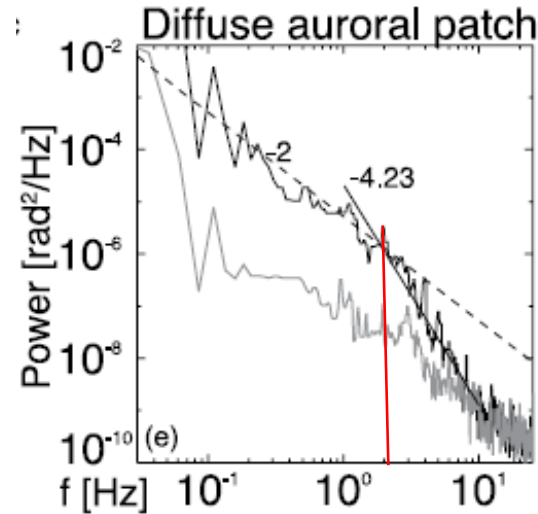
The number of free electrons along a path between a signal transmitter and receiver.

The electrons cause the signal to refract as it travels through the ionosphere.

- This refraction interferes with the signal's path, causing a delay in the time from the transmitter to the receiver.
- This delay makes GPS systems less accurate.



Fresnel frequency: The frequency at which signals interacting with an obstruction will diffract, causing increased signal noise and loss.



$$f_F = \frac{v_{TID}}{r_F}$$

$$r_F = \sqrt{n\lambda d_{rec}}$$

$r_F \equiv$ Fresnel radius

$f_F \equiv$ **Fresnel frequency**

$v_{TID} \equiv$ Propagation speed

$\lambda \equiv$ Signal wavelength

$d_{rec} \equiv$ TID to receiver distance




CASES Capabilities and Data Logging

ASTRA's Space Weather Monitor

Science
Technology
Applications
Bringing It All Together

CASES On-Board Data Products

	Per Channel High Rate	Per Channel Low Rate	Scintillation Params	Navigation Solution
Default Rate	100 Hz	1 Second	100 Second	1 Second
Configurable Rate?	Yes 50 or 100 Hz	Yes >= 1 Second	Yes	Yes >= 1 Second
Parameters	I's, Q's, Integrated Carrier Phase	Pseudorange- based TEC	S4, σ_{ϕ}, T₀	Position Velocity
		Phase-based Delta-TEC	Scint. Power Ratio	
		Integrated Carrier Phase		
		Pseudorange		
		Doppler Frequency		





Statement

The goal of this project is to install a distributed sensor array on West Point to provide meaningful ionospheric TEC, phase scintillation, and amplitude scintillation data and analysis in a mid-latitude region. The reason this is important is because minimal study of the mid-latitude ionosphere has been conducted, and it is the atmospheric region under which the majority of military and U.S. civilian operations are done. Additionally, using this research and network, atmospheric and remote sensing courses will be created for cadets.

Purpose

Can a distributed system of ionospheric sensors be installed, at a relatively low cost, to measure the TEC, amplitude scintillations, and phase scintillations in the ionosphere over a mid-latitude site to characterize the ionosphere.



The Application of Spherical Elementary Current Systems (SECS)

$$\nabla \times \vec{B} = \mu_0 \vec{J} + \cancel{\mu_0 \epsilon_0} \frac{\partial \vec{E}}{\partial t} : \text{Ampere-Maxwell Law}$$

$$B(r) = \int G(r, r') J(r') dV' : \text{Green's Function}$$

Horizontal Currents

$$G_B(\theta, \varphi) = \frac{I}{4\pi R} \frac{1}{\sin\theta}$$

Field Aligned Currents

$$G_h(\theta, \varphi) = \frac{I}{4\pi R} \frac{1}{\sin\theta} \hat{e}_\varphi$$

$J = G^{-1}B$ – Solving for the Currents Strength

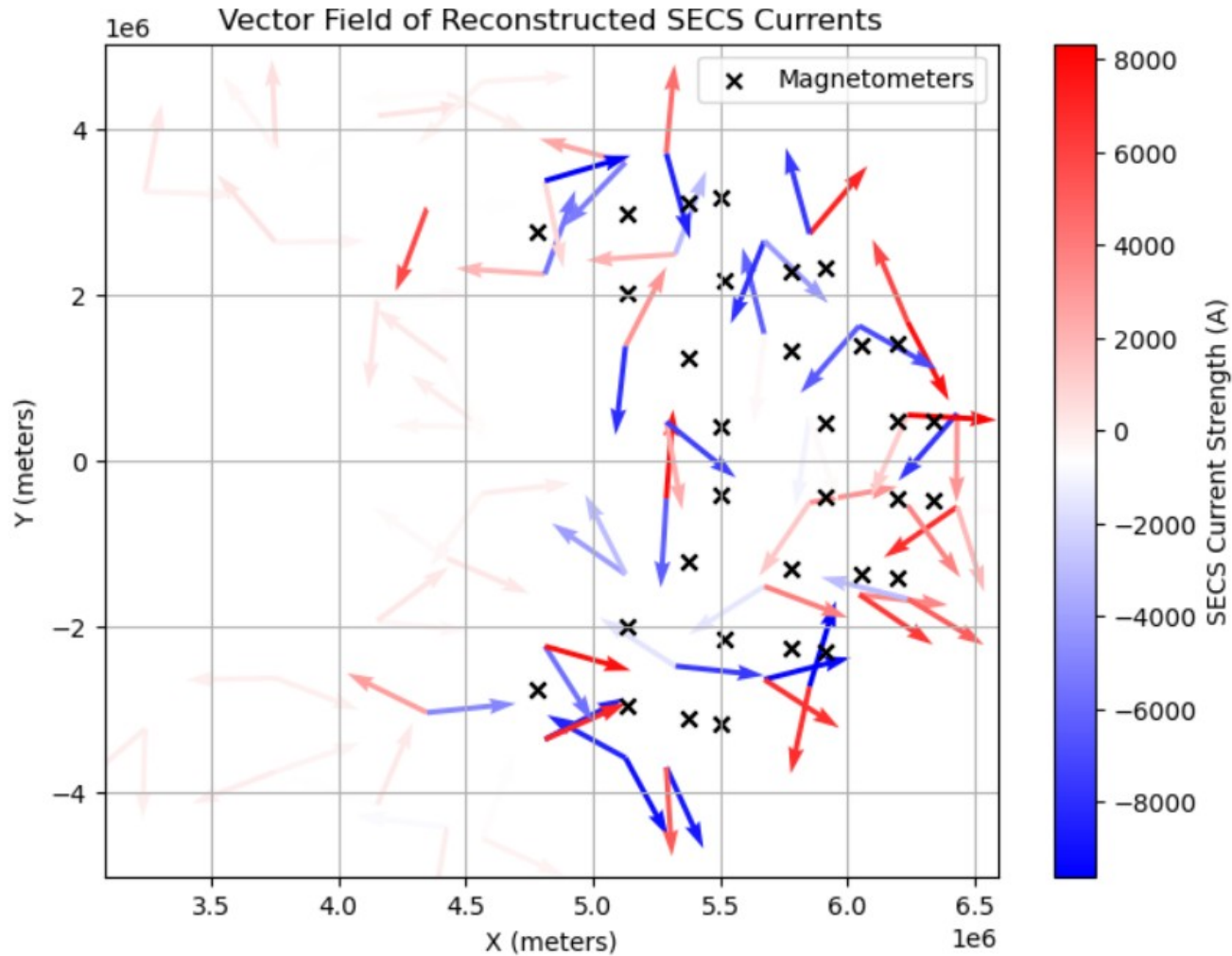


Assumptions, Pros, and Cons of SECS

- The ionosphere is assumed to be a uniform sheet at 110km
- An array of nodes gives reference points over the sensor array of for current reconstruction – these are mathematical points
- Can't differentiate from non-ionospheric sources
 - GIC analysis will need to be conducted
- Requires multiple sensors free of electromagnetic disturbances
- Pros
 - The sensor location can be irregular
 - Scalable Spatial Resolutions
 - Characterizes regional currents
- Cons
 - Only a 2D rendition of or currents, can't determine vertical structure
 - Can't account for fast fluctuations from geomagnetic storms

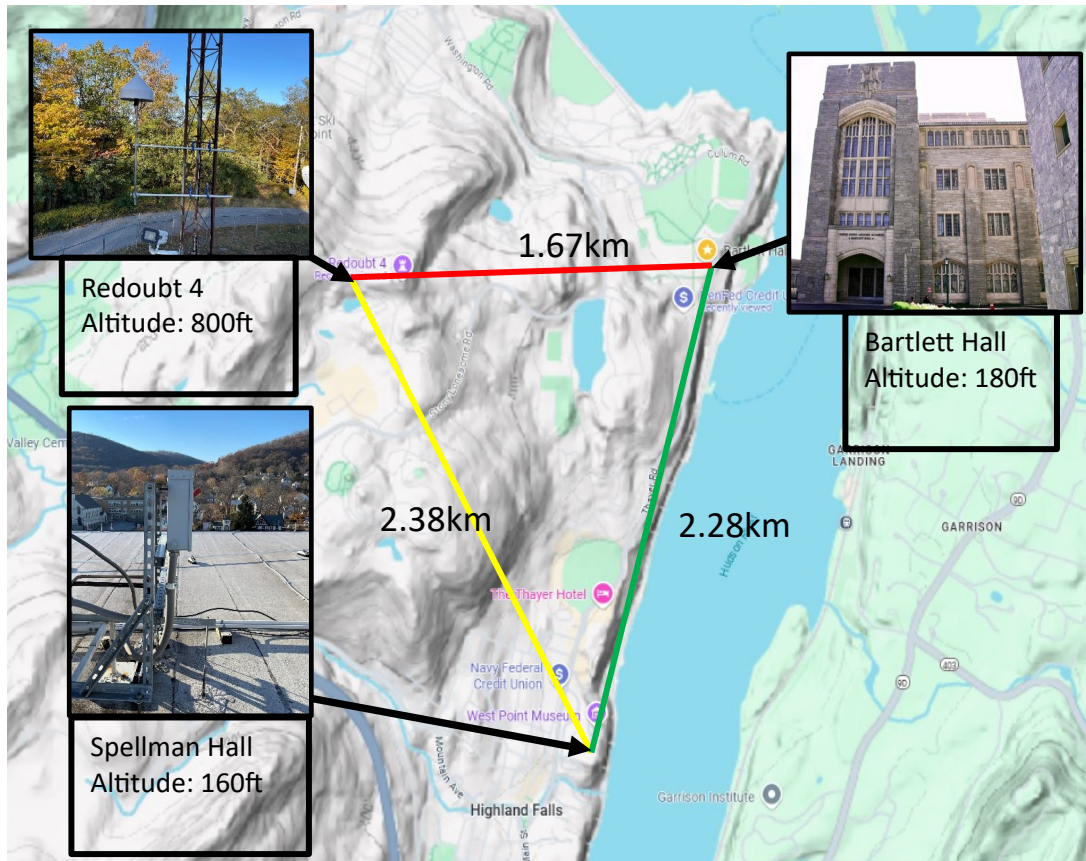


Simulation Of Code





Installation Process



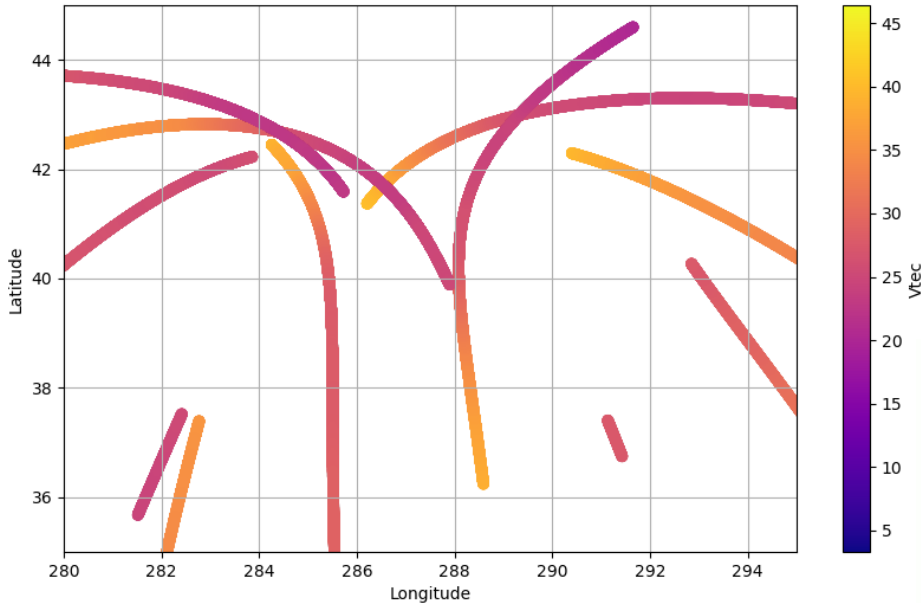
What's the difference between environmental sensors and sies/electrometers?

1. Installed: 3 x GPS receivers
2. Pending requisition and installation:
 1. Magnetometers and Environmental Sensors
 2. Seismometer
 3. Electrometer

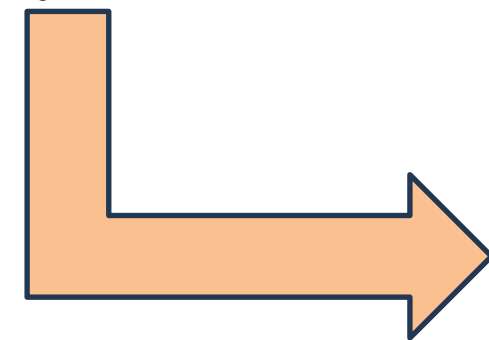


Propagation Speed Derivation Methodology

First Data Window: Scatter Plot of Vtec Values

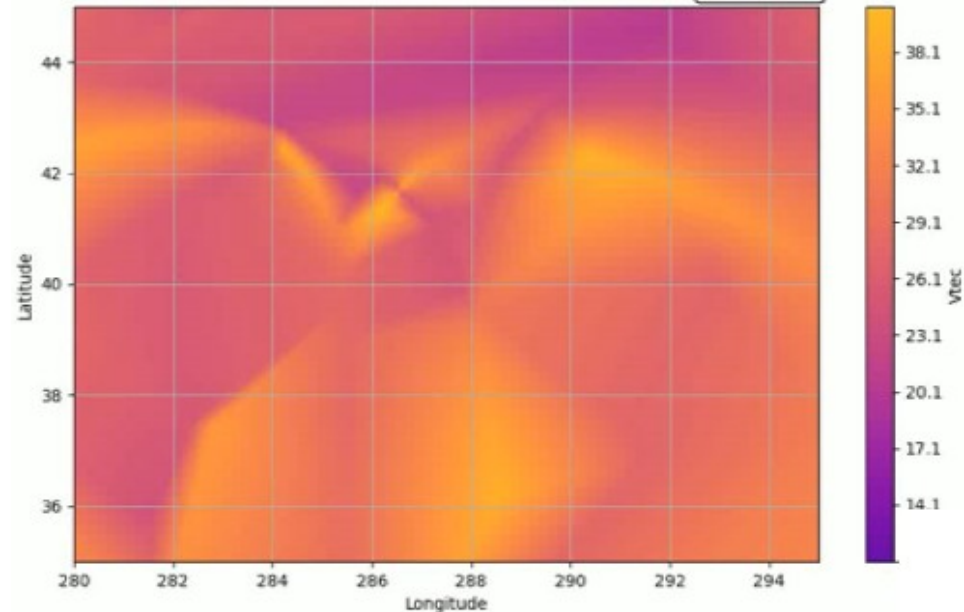


- VTEC Data unbiased by CDT Halfhill
- 4-Hour binning with 15-minute step
- ~500km radius of view
 - > 1 million kilometers of area



**Linear Interpolation
between data points**

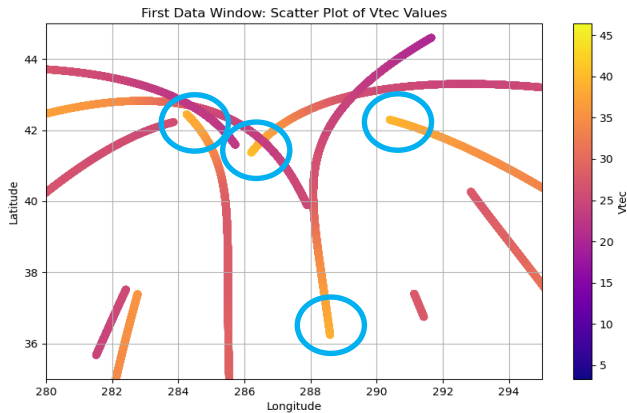
Heatmap of Vtec Values
EST: -5:00





Propagation Speed Derivation Methodology (Cont'd)

Step 1: Identify maxima in time bin-1



Step 2: Log time bin-1 maxima information

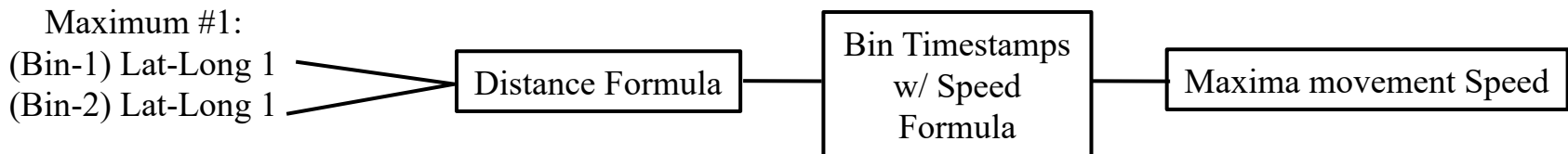
Maximum	vTEC	Location
#1	1 st Highest	Lat-Long 1
#2	2 nd Highest	Lat-Long 2
#3	3 rd Highest	Lat-Long 3
#4	4 th Highest	Lat-Long 4

Step 3: Repeat steps 1-2 for time bin-2

Step 4: Calculate straight line distance between maxima from bin-1 to bin-2 in rank order

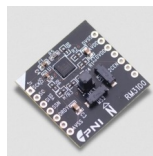
Step 5: Repeat step 4 for all maxima in bins and average results.

Step 6: Repeat step 1-5 for Bin-2 and Bin-3, Bin-3 and Bin-4, etc. Average the results over desired time period to get TID propagation speed

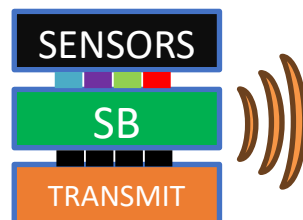




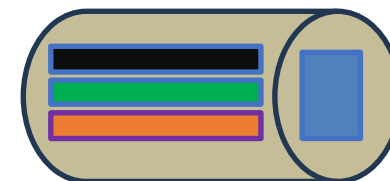
STEP 1:
Run RM3100 and other sensors on standard microcontroller, start programming. (SPI/I2C)



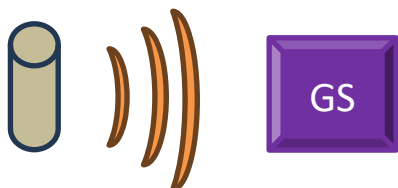
STEP 2:
Start work with LoRaWAN Gateways. Set up remote indoor operation with sensor board and transmitter.



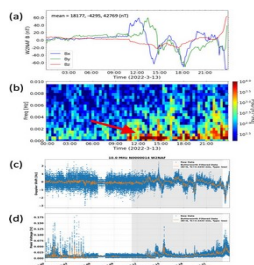
STEP 3:
Design a weatherproof enclosure for the components. Integrate solar panel and battery.



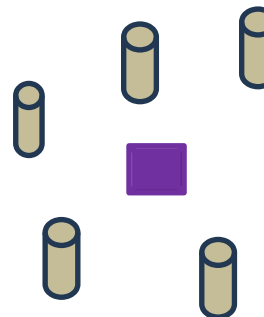
STEP 3:
Install node in tested outdoor location, set up link with rooftop ground station.



STEP 4:
Test the system and hardware, monitor results remotely.



STEP 5: Repeat, Build a Network of Nodes.



STEP 6: Crowdsource data with HAMSCI Network/Web Server/Machine Learning Algorithm





- 1) Datta-Barua, S., Su, Y., Deshpande, K., Miladinovich, D., Bust, G. S., Hampton, D., and Crowley, G. (2015), First light from a kilometer-baseline Scintillation Auroral GPS Array. *Geophys. Res. Lett.*, 42, 3639–3646. doi: 10.1002/2015GL063556.
- 2) GISGeography. “How GPS Receivers Work - Trilateration vs Triangulation.” GIS Geography, 31 May 2022, gisgeography.com/trilateration-triangulation-gps/.
- 3A) “Plasma Interactions.” *The Space Environment and Its Effects on Space Systems*, by Vincent L. Pisacane, 2nd ed., American Institute of Aeronautics and Astronautics, 2016, pp. 615–621.
- 3B) Vertical Value of Total Electron Content (VTEC) Obtained ... - Researchgate. www.researchgate.net/figure/Vertical-value-of-total-electron-content-VTEC-obtained-from-STECSOURCE-THAI-GNSS-AND-FIG1-351099620.
- 4) Crowley, Geoff. “ASTRA Realtime Space Weather Operations.” *astraspace.net*, www.swpc.noaa.gov/sites/default/files/images/u33/EffectsofSpaceWeatheronGPS_GeoffCrowley_ASTRA.pdf. Accessed 19 Nov. 2023.
- 5) Skolnik, Merrill I. "radar". *Encyclopedia Britannica*, 17 Aug. 2024, <https://www.britannica.com/technology/radar>. Accessed 13 September 2024.
- 6A) Yuhao Zheng, Chao Xiong, Yaqi Jin, Dun Liu, Kjellmar Oksavik, Chunyu Xu, Yixun Zhu, Shunzu Gao, Fengjue Wang, Hui Wang and Fan Yin J. *Space Weather Space Clim.*, 12 (2022) 40. DOI: <https://doi.org/10.1051/swsc/2022036>
- 6B) Chen, C.H., Saito, A., Lin, C.H. et al. Medium-scale traveling ionospheric disturbances by three-dimensional ionospheric GPS tomography. *Earth Planet Sp* 68, 32 (2016). <https://doi.org/10.1186/s40623-016-0412-6>
- 6C) Jiang, H.; Jin, S.; Hernández-Pajares, M.; Xi, H.; An, J.; Wang, Z.; Xu, X.; Yan, H. “A New Method to Determine the Optimal Thin Layer Ionospheric Height and Its Application in the Polar Regions.” *Remote Sensing*. 2021, 13, 2458. <https://doi.org/10.3390/rs13132458>
- 6D) Nishimura, Y., T. Kelly, P. T. Jayachandran, S. Mrak, J. L. Semeter, E. F. Donovan, V. Angelopoulos, and N. Nishitani. 2023. “Nightside High-Latitude Phase and Amplitude Scintillation During a Substorm Using 1-Second Scintillation Indices.” *Journal of Geophysical Research Space Physics* 128 (8). <https://doi.org/10.1029/2023ja031402>.
- 7) Vanhamäki, Heikki & Juusola, Liisa. (2019). Introduction to Spherical Elementary Current Systems. 10.1007/978-3-030-26732-2_2.



- 8A) Amm, O., and A. Viljanen (1999), Ionospheric disturbance magnetic field continuation from the ground to ionosphere using spherical elementary current systems, *Earth Planets Space*, 51, 431–440.
- 8B) Building the SAM-III Fluxgate Magnetometer | Space Science Center. (2022, December 23). UNH Earth, Oceans, & Space. <https://eos.unh.edu/space-science-center/outreach/space-weather-underground/building-sam-iii-fluxgate-magnetometer>. *Data Types Information | Space Weather Lab at IIT*. <https://apollo.tbc.iit.edu/~spaceweather/live/?q=pfrr/data-types-information>.
- 8C) Frissell, N. A., Kaeppler, S. R., Sanchez, D. F., Perry, G. W., Engelke, W. D., Erickson, P. J., et al. (2022). First observations of large scale traveling ionospheric disturbances using automated amateur radio receiving networks. *Geophysical Research Letters*, 49, e2022GL097879. <https://doi.org/10.1029/2022GL097879>
- 9) Griffiths, David J. *Introduction to Electrodynamics*. 4th ed. Cambridge: Cambridge University Press, 2017. Print.
- 10) Harris, S.E., Mende, S.B., Angelopoulos, V. et al. THEMIS Ground Based Observatory System Design. *Space Sci Rev* 141, 213–233 (2008). <https://doi.org/10.1007/s11214-007-9294-z>
- 11) Juusola, L., K. Kauristie, H. Vanhamäki, A. Aikio, and M. van de Kamp (2016), Comparison of auroral ionospheric and field-aligned currents derived from Swarm and ground magnetic field measurements, *J. Geophys. Res. Space Physics*, 121, 9256–9283, doi:10.1002/2016JA022961.
- 12A) Kim, H., Witten, D., Madey, J., Frissell, N., Gibbons, J., Engelke, W., Liddle, A., Muscolino, N., Visone, J., & Cao, Z. (2024). Citizen science: Development of a low-cost magnetometer system for a coordinated space weather monitoring. *HardwareX*, 20, e00580. <https://doi.org/10.1016/j.ohx.2024.e00580>
- 13) Merkin, Dr. Viacheslav, "NASA DRIVE Science Center for Geospace Storms: Transforming the Understanding and Predictability of Space Weather". UNH Space Science Center Seminar, 22 Sep 2022, <https://www.youtube.com/watch?v=eIvQf8oq1Is>
- 14) PNI Sensor Corporation. (n.d.). RM3100: 3D magnetometer sensor. PNI Sensor Corporation. Retrieved November 21, 2024, from <https://www.pnisor.com/rm3100/>
- 15A) R. Pirjola, "Geomagnetically induced currents during magnetic storms," in *IEEE Transactions on Plasma Science*, vol. 28, no. 6, pp. 1867-1873, Dec. 2000, doi: 10.1109/27.902215.



- 15B) Ritter, P., Lühr, H. & Rauberg, J. Determining field-aligned currents with the Swarm constellation mission. *Earth Planet Sp* 65, 1285–1294 (2013). <https://doi.org/10.5047/eps.2013.09.006>
- 16) Rodrigues, F. S., Socola, J. G., Moraes, A. O., Martinis, C., & Hickey, D. A. (2021). On the properties of and ionospheric conditions associated with a mid-latitude scintillation event observed over southern United States. *Space Weather*, 19, e2021SW002744. <https://doi.org/10.1029/2021SW002744>
- 17) Vanhamäki, Heikki & Juusola, Liisa. (2019). Introduction to Spherical Elementary Current Systems. 10.1007/978-3-030-26732-2_2.